J. Radiat. Res., 51, 441–448 (2010)

Regular Paper

Monte Carlo Simulation of Average Glandular Dose and an Investigation of Influencing Factors

Khatayut NIGAPRUKE[1]*, Patana PUWANICH[1], Nakorn PHAISANGITTISAKUL[2] and Wiwat YOUNGDEE[1]

Average glandular dose/Monte Carlo simulation/Mammography/Glandular distribution.

This study aims to determine the average absorbed dose of radiation in glandular tissue during mammography and to investigate factors that influence the average glandular dose, particularly the local distribution of glandular tissue within the breast and breast skin thickness. An EGSnrc Monte Carlo code and associated codes were employed in the simulation. The breast voxel models used consist of a homogeneous and heterogeneous mixture of adipose and glandular tissues embedded in a skin layer. The percent depth dose and normalized average glandular dose coefficients for spectra of Mo-Mo target-filter combination were calculated. The results showed good agreement with the experimental results (percent depth dose) and literature values (normalized average glandular dose coefficients) when the breast model is homogeneous. Additional investigation of a heterogeneous breast phantom indicates that the local distribution of glandular tissue within the breast, as well as breast skin thickness, could affect the average glandular dose considerably more than that of a typical homogeneous breast model. This problem may be a concern in most practical situations of breast dosimetry when assessing the radiation risk to patients.

INTRODUCTION

Recently, the use of mammography has increased rapidly worldwide for detecting breast cancer in women. Because the glandular tissue in the female breast is regarded as a radiosensitive organ, breast dosimetry is considered to be an important basis for the assessment of radiation risk to glandular tissue for patients undergoing mammography.[1–3] The average dose absorbed in the glandular tissue, called the average glandular dose, is preferred for radiation risk assessment. The average glandular dose (AGD) is the energy deposited per unit mass of glandular tissue averaged over all of the glandular tissue in the breast.[4] Monte Carlo simulation models have been widely used for a precise determination of the average glandular dose absorbed in the breast.

By using a Monte Carlo (MC) simulation, the normalized glandular dose coefficients (DgN) can be derived by dividing the average glandular dose in the irradiated breast volume by the incident air kerma (K_i) at the breast surface (without backscattering). The computation method used to determine the DgN values as a function of radiation quality, breast thickness, and breast composition has been described in previous works.[1–3,5,6] In addition, other factors that can influence the DgN calculations have also been evaluated, including the radiation transport code, photon spectra, tissue composition, cross section data, backscattering materials, superficial (skin) layer (tissue composition and thickness), and presence and absence of a compression plate.[2,7,8]

Most published works have reported DgN values that are based on a homogeneous breast model, while data of DgN values for a heterogeneous breast model are sparse.[1–3,5,6] A heterogeneous breast model can be created from a variety of mathematical geometries[9] or from segmented voxel data.[10] In addition, some parameters involved in the calculation of the DgN, such as skin thickness and tissue composition, breast shape and size, and thickness of breast support, should be also investigated further.

The purpose of the present work was to calculate the DgN values for both breast models and to investigate some of the above-mentioned factors that influence the calculated DgN. A Monte Carlo method was employed in the present work because it is a useful tool for accurate and precise simulation of radiation transport in a mathematical breast model. To validate the MC simulation procedure used, we compared the simulated results of the depth dose distribution deposited

*Corresponding author: Phone: +66-0-4220-7367,
Fax: +66-0-4220-7367,
E-mail: khatayut.n@dmsc.mail.go.th

[1]Department of Physics, Faculty of Science, Khon Kaen University, Thailand; [2]Department of Physics, Faculty of Science, Chulalongkorn University, Thailand; [2]ThEP center, CHE, 328 Si Ayutthaya Road, Ratchathewi, Bangkok, Thailand.

doi:10.1269/jrr.10008

inside the breast tissue-equivalent phantom with those of TLD experiments,[11–13] and some of the calculated DgN values were also compared with literature values.

MATERIALS AND METHODS

Patient breast data survey

To determine the breast dimensions for a sample group in Thailand, we used survey data with 371 representative samples of breasts from women in four hospitals that conduct mammography screenings. However, in the present work, we gathered the patient-related data only for the cranio-caudal projection view, which will be used next in the simulation of a breast model. The obtained survey data were summarized as follows: the average age of the patients was about 46 years (range: 28 to 72 years of age), the average breast size was 15.5 ± 2.9 cm for a lateral-to-lateral distance and 6.6 ± 1.8 cm for a chest wall-to-nipple distance, the average breast thickness was 4.4 ± 0.7 cm, the average tube voltage was 25 ± 1 kV, and the average tube current-exposure time product was 131 ± 23 mAs.

Monte Carlo simulation

The computer simulation, running on RedHat Linux Version 9.0, involves two stages as follows. In the first stage, the detailed components of the mammography systems, a Lorad mammography unit (model M-IV; Lorad Medical Systems, Inc.), were modeled by using the EGSnrc/BEAMnrc Monte Carlo code system.[14] A parallel rectangular monoenergetic beam (0.3 mm × 0.3 mm) of 1×10^8 electrons was transported to an X-ray tube target (angle of 16°) with an electron cut off energy (ECUT) of 516 keV and a photon cut off energy (PCUT) of 5 keV. The irradiation field size was 18 cm × 24 cm for all simulations. Further details of the simulation have been described in a previous work.[15] In the present work, the spectra of Mo-Mo (30 μm) target-filter combination were generated at tube voltages of 23, 25, 27, 29, and 31 kV, respectively. At a given tube voltage, different half-value layers (HVLs) were obtained by adding layers of polymethylmethacrylate (PMMA) from 1 to 5 mm; a 3-mm-thick PMMA layer typically represents a compression plate. The acquired spectral data were then employed in the second stage of the simulation.

Subsequently, in the second stage of the simulation, the EGSnrc/DOSXYZnrc code system[16] was employed to calculate the dose absorbed in a three-dimensional voxel phantom. The phase space data, information concerning particles included the position, direction, charge, energy, weighting, and origin (LATCH), obtained from the previous mammography simulation are used as the source data for this part of the simulation. To reduce the computing time without losing precision, both the ECUT and PCUT values were set to the same values used in the BEAMnrc simulation, and the range rejection option was enabled, with the ESAVE value set to 517 keV. To increase the efficiency of the dose calculation, the photon splitting number was invoked as a variance technique (i.e., the parameter n_split = 2). During the sampling by the DOSXYZnrc code, the particles were redistributed symmetrically (i.e., the parameter ISMOOTH = 1) when they were used more than once.

We created a phantom model using the DOSXYZnrc code for any size or simple geometric shape by defining the voxel dimensions in the x, y, and z directions, and the voxel spatial resolution in the peripheral edge portion of the phantom can be improved by using small voxel dimensions and increasing the number of voxels. The breast model was assumed to have a semielliptical cylindrical shape for the compressed breast in the cranio-caudal projection, with the central region of the phantoms consisting of a homogeneous mixture of adipose and glandular tissues contained within a skin layer.[3] The typical geometry of the breast model simulation is shown in Fig. 1. Based upon the survey data described above, the cross section of a simple breast model that comprises a half ellipse with a minor axis (lateral-to-lateral distance) of 16 cm and a semi-major axis (chest wall-to-nipple distance) of 7 cm was considered, along with a 4-mm-thick skin layer based on published data. The materials and the corresponding densities, according to ICRU Report No. 44,[17] employed in most simulations were created with the PEGS4 program. PEGS4 data set is based on XCOM photon cross section compilations.[18] The mass energy absorption coefficients used in the calculation were taken from the National Institute of Standards and Technology (NIST) data base.[19]

Normalized glandular dose

The DgN values for a homogeneous mixture breast consisting of 50% glandular and 50% adipose tissue and one of 0% glandular were computed by using the glandular weighting factor defined in the work of Liu *et al.*[6] and using Equation (6) of Boone[2] to correct the obtained DgN values for only the dose absorbed in the glandular tissue component. Note that this correction is not necessary for 100% glandular tissue. In the present work, the DgN values were computed in mGy/mGy; however, we can convert to the conventional unit of mrad/R by multiplying the factor of 8.764 and a given unit of mGy/mGy.

Comparison of DgN with values reported in the literature

To benchmark the EGSnrc MC code system with another code, that is, the MCNP code reported in the work of Wu *et al.*[3] and the TART97 code used in the work of Boone,[2] we employed a breast geometry and beam qualities that are similar to those of both Wu *et al.*[3] and Boone.[2] The DgN values were calculated as a function of tube voltage (varying from 23 to 31 kV at 2-kV increments), breast composition (a homogeneous mixture of 100% glandular, 50% glandular

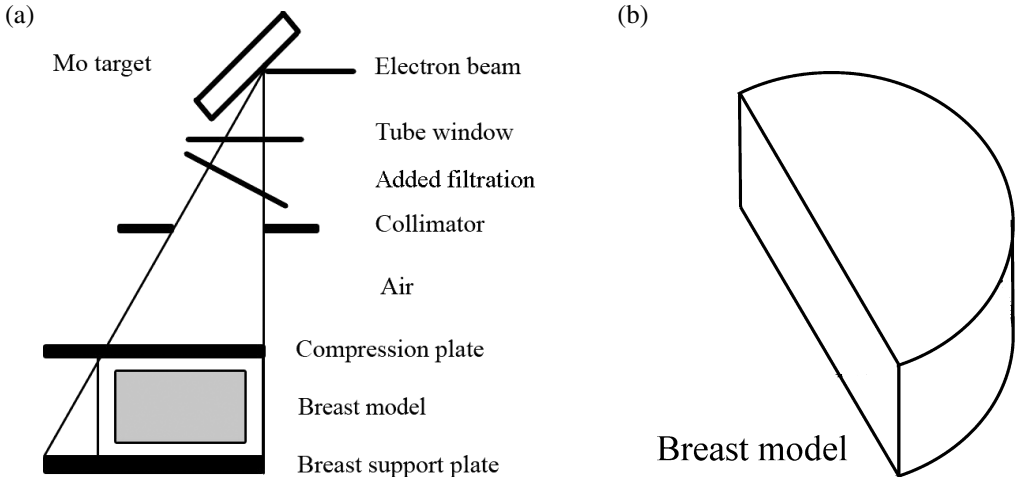

Fig. 1. (a) Schematic representation of the breast irradiation geometry (not to scale) including the compression plate and the breast support plate. The breast model in the cranio-caudal projection; the central region represents a mixture of glandular and adipose tissues, and the outer region represents the skin layer. (b) Schematic of the semielliptical breast model that enclosed with the skin layer.

and 50% adipose tissue, and 0% glandular tissue), and breast thickness (varying from 3 to 8 cm at 1-cm increments). All simulations were carried out by using only the spectra of Mo-Mo target-filter combination, which are adequate for assessing the validation of the simulations with the EGSnrc code system.

Factors influencing the estimation of DgN

In this section, the influence of variation in some important factors affecting the estimation of the DgN values using the 25-kV Mo-Mo spectrum was investigated in additional models, including glandular distribution in the breast, skin thickness and tissue composition, breast shape and size, and thickness of breast support.

To assess the effect of the glandular distribution in the breast on the DgN values, a 4.8-cm-thick heterogeneous (tissue) breast phantom was created by using a number of contiguous slabs of pure glandular tissue that can vary in thickness in order to obtain the desired glandular fraction of 25%, 50%, and 75% and by placing them at different positions in the pure adipose (tissue) breast phantom. For modeling of a 25% glandular breast, a 1-cm-thick glandular slab was positioned at 7, 12, 17, and 22 mm below the cranial surface of the breast. For modeling of a 50% glandular breast, a 2-cm-thick glandular slab was positioned at 12, 17, and 22 mm below the cranial surface of the breast. For modeling of a 75% glandular breast, a 3-cm-thick glandular slab was positioned at 17 and 22 mm below the cranial surface of the breast.

Furthermore, different types and thicknesses of breast skin layers were also studied. The composition data of adipose and skin tissues from both Hammerstein *et al.*[20] and ICRU Report No. 44[17] were used. The skin thickness was varied from 2 to 6 mm, corresponding to the z-axis voxel dimension. However, the energy absorbed in the skin and the mass of the skin are not included in the calculation of the glandular dose because the carcinogenic risk in the skin is considered minimal.[6] To assess the effect of the breast shape on glandular dose, we constructed additional breast models in two shapes as follows: a semicircular cylinder shape with dimensions of $14 \times 7 \times 4$ cm^3 and a rectangular cube shape with dimensions of $14 \times 14 \times 4$ cm^3, with voxel dimensions of $5 \times 5 \times 5$ mm^3. In addition, two breast sizes ($22 \times 12 \times 4$ cm^3 and $13 \times 4 \times 4$ cm^3) of semielliptical shape were also modeled. Finally, backscattering material (breast support or image receptor) with a thickness of 5, 10, and 15 mm of PMMA was included in the simulations.[7]

Verification of the EGSnrc MC code

Measurement of the depth dose distribution

To verify our MC simulation, we calculated central axis depth dose curves[12,13] and lateral (on the X-Y plane) depth dose curves for a 4-cm BR12 phantom (Gammex rmi, Middleton, WI), which has X-ray properties similar to those of a mixture of 50% glandular and 50% adipose tissue by weight, for 25 kV of Mo-Mo target-filter combination with a measured HVL value of 0.32 mm Al. We then compared the results to experimental values obtained using thermoluminescent dosimeters (TLDs).[11]

Depth dose curves were obtained by measuring the dose with depth in a phantom for a given energy and field size. The dose at various depths was then normalized to the dose maximum, which occurs at the phantom surface and on the central axis of the X-ray beam, and a plot of relative dose versus depth in the phantom was produced. The depth dose curves were measured by placing calibrated TLD-100H

(LiF:Mg,Cu,P) chips ($3 \times 3 \times 0.9$ mm^3) at different depths in a breast tissue-equivalent material (BR12 phantom) and exposing them to low-dose X-ray mammography with a 25-kV beam for a field size of 18 cm × 24 cm that encompassed the 14 cm × 14 cm BR12 slabs with differences in thickness from 0.5 to 2 cm in 0.5-cm steps. These slabs were stacked to obtain the desired thickness. To minimize the air gap between the phantom slabs and to obtain the dose distribution, hole patterns for TLD placement along the x- and y-axes (in the direction parallel and perpendicular to the anode-cathode axis) were drilled into the surface of the phantom, accommodating the chip-shaped TLDs, and the spacing between the center of each hole was 2 cm. For the measurements, the phantom loaded with TLDs was positioned in the center of the image receptor, as in typical clinical examination situations. The TLDs were then integrated for three exposures of 25 kV to increase the TLD signals, thus reducing the statistical uncertainty of the results.

RESULTS

Verification of the EGSnrc MC code

The results of the MC calculation of the relative dose distribution in the breast phantom in terms of central axis depth dose curves and lateral depth dose profile curves were compared with those of experimental measurements with TLDs and are presented in Figs. 2a and b, respectively. Both the calculated and measured depth dose curves were normalized to a depth of 0 cm (on the surface) for the dose maximum. All TLD depth dose data except for that at 0 cm were corrected for the energy dependence caused by beam hardening in the BR12 material.

Figure 2a shows that good agreement of the central axis depth dose curves was observed between the MC simulation and TLD measurement, except that the measurement curve was slightly higher at greater depths. The maximum relative error between these curves was less than 4%, and the maximum standard deviation for the TLD measurement was about 4%. An evidence of the Heel effect was generally observed for the lateral depth dose profiles against distance along the x-axis (Fig. 2b), which the depth dose curves on cathode side (+x) was higher than that of on anode side (–x) by about 6%, 3%, 1%, and 0.1 for depths at 0, 0.5, 1.5, and 3.5 cm, respectively. An obvious fluctuation in the TLD depth dose values was found especially for depths from the surface to 0.5 cm (relative error was less than 3%), and the MC depth dose curves tend to be slightly less than the TLD depth dose data for greater depths at 1.5 to 3.5 cm (relative error was less than 2%). In addition, both end portions of the curves tend to be lower than the middle portion. We also simulated a lateral depth dose profile against distance along the y-axis, in which the Heel effect does not occur at all, and similar curve trends were evident in both profiles.

Comparison of DgN with literature values

The DgN values calculated for a breast with a glandular fraction of 100% were compared with the results of the previously published works of Wu *et al.*[3] and Boone,[2] as shown in Figs. 3a and b. For comparison with other works, the DgN values are expressed in units of mrad/R.

Although the DgN values for 50% and 0% glandular were calculated only the DgN values for 100% glandular breast are presented (Figs. 3a and b). In general, the DgN values for 100%, 50% and 0% glandular in the present work agree with those of Wu *et al.*[3] and Boone.[2] Figure 3a shows that the DgN values increase, at a factor of about 1.05 per 1 kV,

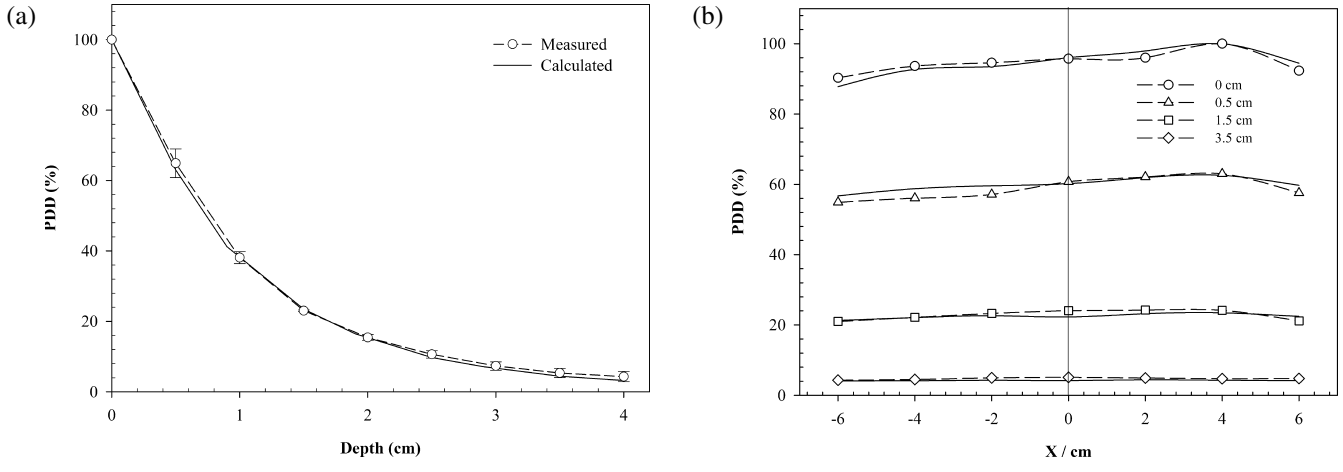

Fig. 2. Percent depth dose (PDD) in a 4-cm homogeneous breast phantom is expressed as: (a) Central axis depth dose as a function of depth and (b) Lateral depth dose profiles as a function of depth at 0, 0.5, 1.5, and 3.5 cm and of distance along the x-axis (parallel to the anode-cathode direction) from -6 to 6 cm. By using a tube voltage of 25 kV for a Mo-Mo target-filter combination and a compression plate; an irradiated field size of 18 cm × 24 cm. The solid lines refer to the Monte Carlo calculated data, and the dotted lines with open symbols refer to measured data.

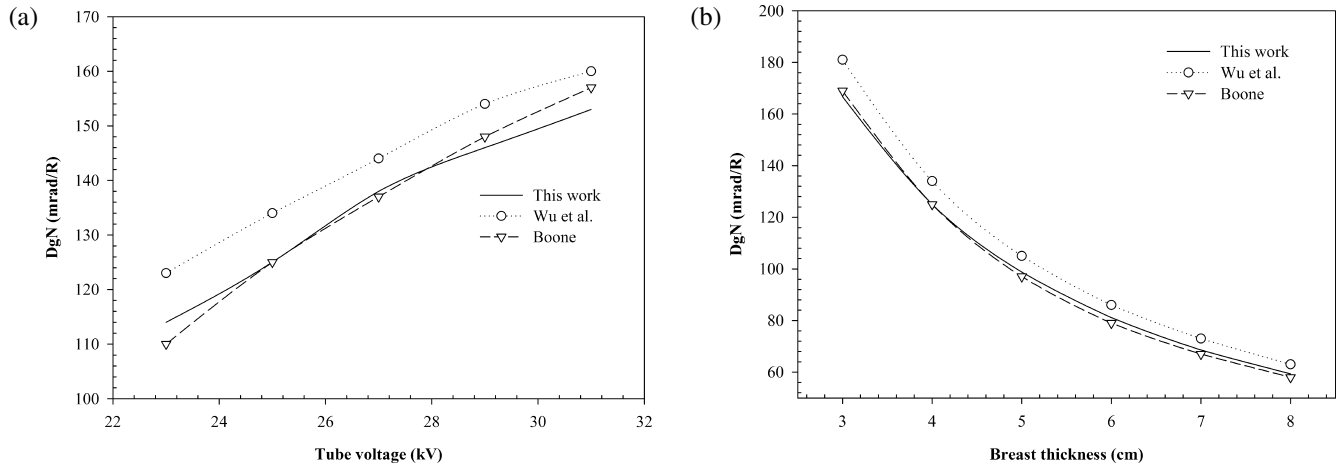

Fig. 3. Comparison of the calculated DgN values with literature values as a function of: (a) Tube voltage of 23, 25, 27, 29, and 31 kV (fixed at 4-cm-thick breast) and (b) Breast thickness of 3 to 8 cm (fixed at 25 kV). The simulations for both (a) and (b) use a breast phantom of 100% glandular fraction with a Mo-Mo anode-filter combination and a compression plate, as in clinical settings.

as the voltage increases from 23 to 31 kV (corresponding to a calculated half value layer of 0.310, 0.328, 0.345, 0.359, and 0.372 mm Al, respectively) for a 4-cm-thick 100% glandular breast. We found that the DgN values in this work are lower than the results of Wu *et al.*[3] by about 7%, while they differ slightly from the results of Boone[2] by between –3% to 4%. For the DgN expressed as a function of breast thickness, Fig. 3b shows that the DgN values decrease, at a factor of about 1.3 per 1 cm, as the thickness increases from 3 to 8 cm, for 100% glandular breast with the 25-kV Mo-Mo spectra. Comparing to other works, our DgN values are slightly greater than those of Boone by about 3% for all of the breast compositions, including 50% and 0% glandular breasts, but they are noticeable lower than those of Wu *et al.*[3] by about 7%, 8% and 12% for 100%, 50% and 0% glandular breasts, respectively. It was found that the DgN values increase when glandular fraction decrease from 100% to 0% in which the ratio between glandular fraction of 100% to 50% and 100% to 0% are 1.3 and 1.5, respectively.

Factors influencing the estimation of DgN

Glandular distribution in the breast

As expected, a wide variation of the DgN values was observed in each group of glandular fractions of 25%, 50%, and 75% with the same tendency, as shown in Fig. 4a. The DgN values dramatically decrease when the center position of the slabs was moved from the upper part to the lower part of the breast. The variability in DgN values (Fig. 4a) with different center positions, when compared with the maximum values at the uppermost part of the breast, was found to range from –53% to –88%, –52% to –76%, and –52% (one position) for glandular fractions of 25%, 50%, and 75%, respectively. In comparing the DgN values for the same glandular fraction from homogeneous tissue breast model data and from heterogeneous tissue breast model data, a large of discrepancy of the DgN values was revealed (Figs. 4a and b); the difference in those DgN values, when compared with the values of a homogeneous tissue breast, was found to range from 96% to –76%, 45% to –65%, and 17% to –43% for glandular fractions of 25%, 50%, and 75%, respectively.

Skin thickness and tissue composition

For the tissue composition given in ICRU Report No. 44,[17] the influence of skin thickness and type of superficial layer on the DgN value is illustrated in Fig. 5. In general, the DgN values decrease with increasing superficial thickness, while the skin tissue has a larger variation on the dose than adipose tissue. The results showed that the DgN values obtained for adipose tissue are higher than for skin tissue, ranging from 11% to 27% as the layer thickness increases from 2 to 6 mm.

We employed the breast and skin tissue composition data reported in the work of Hammerstein *et al.*[20] and ICRU Report No. 44.[17] We found that using the data from Hammerstein *et al.*[20] resulted in DgN values that are slightly higher than those obtained using the ICRU Report No. 44[17] data by about 2% for breast tissue and 0.7% for skin tissue.

Breast shape and size

Three breast shapes, consisting of semielliptical cylindrical, semicircular cylindrical, and rectangular cube shapes, for the cranial-caudal projection view of the compressed breast were modeled, and the dose absorbed was investigated in these breast models. The results showed that the DgN values differ by less than 0.7% for any breast model shape. To study the effect of breast size on the DgN values, using a semielliptical breast cross section with a chest wall

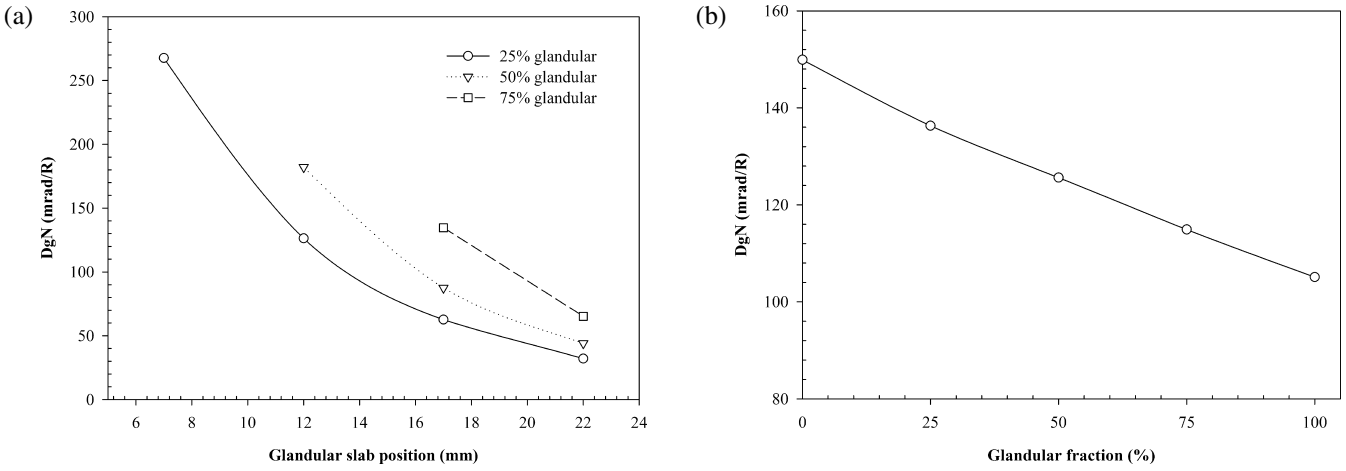

Fig. 4. Comparison of the DgN values for two 4.8-cm-thick breast models: (a) Heterogeneous tissue breast model for glandular fractions of 25%, 50%, and 75% and (b) Homogeneous tissue breast model for glandular fractions between 0% to 100%. All simulations used a tube voltage of 25 kV for a Mo-Mo target-filter combination and a compression plate.

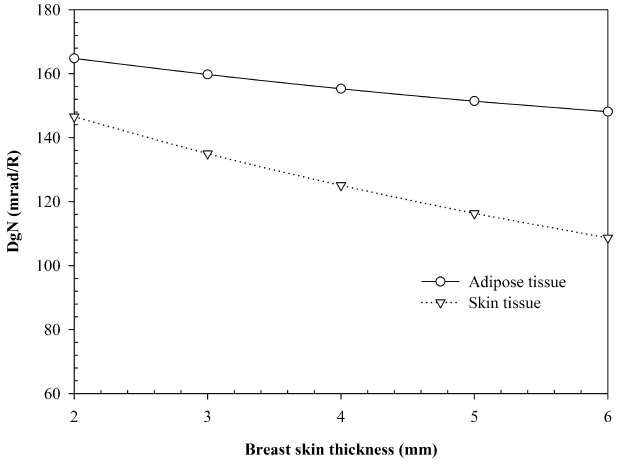

Fig. 5. Comparison of the DgN values as a function of skin thickness between adipose tissue and skin tissue (data taken from ICRU Report No. 44) for 4 cm-thick 100% glandular breast. The simulations used a tube voltage of 25 kV for a Mo-Mo target-filter combination and a compression plate.

dimension of 14 cm and a chest wall-to-nipple dimension of 8 cm, we found that for a larger breast section (22 cm × 12 cm), the DgN values decrease by only 0.3%, and they increase by only 0.4% for a smaller breast section (13 cm × 4 cm).

Thickness of breast support

We found that changing the thickness of the breast support from 0.5 to 1.0 cm and from 0.5 to 1.5 cm increases the DgN values by 0.08% and 0.11%, respectively.

DISCUSSION

Due to the effect of beam hardening in the BR12 material, we found that a mean energy of 25 kV traversing into a 4-cm-thick breast of 50% glandular and 50% adipose tissue can shift from 16.06 to 18.43 keV. Hence, a correction for this effect was applied to the measured depth dose data.

The small difference in the depth dose curves (Fig. 2) may be due to two major reasons. First, we assumed the BR12 material in the simulation to be a mixture of 50% glandular and 50% adipose tissue, whereas the manufacturer's data absorption coefficients for the BR12 material are slightly lower than that of actual breast tissue by about 3%. Second, it should be noted that the first measurement depth in our phantom was limited at 0 cm, so all of the data were normalized to this depth. Fluctuations in the TLD depth dose values at shallow depths may be caused by uncertainty in the TLD measurements, which was estimated to be less than 10%.[21] Although TLDs may not suffer from size effects due to their small size, these chips may still produce inaccurate results because their responses vary rapidly in the low energy range.[22] However, the MC simulation data, which have a dose uncertainty no greater than 4%, do correspond well to the TLD measurements with good accuracy. The lateral depth dose profile curves show less radiation intensity at the border region than at the other regions of the beam, which is a characteristic of the point source radiation that we defined in the simulation and may be due to the lateral escape of radiant energy.[8]

There are several factors in the MC simulation that may contribute to the discrepancy between the results of the present work and those of previously published works,[1–3] as follows. First, it may be caused by differences in, for example, Monte Carlo code, photon cross section data, tissue composition and density, and X-ray spectra. In the work of Wu *et al.*,[3] they used the MCNP Monte Carlo code and photon cross sections that were taken from the Evaluated Nuclear

Data File (ENDF), the tissue composition was taken from the data of Hammerstein *et al*.,[20] and the X-ray spectra are based on the model of Tucker *et al*.[24] Meanwhile, Boone[2] used the TART97 Monte Carlo code and the X-ray spectra obtained by using the mathematic spectral model of Boone *et al*.,[25] and the photon cross section data and the tissue composition are the same as in the work of Wu *et al*.[3] Second, apart from these factors, the use of mass attenuation coefficients from different sources may produce a large error in the results. Third, the obvious differences between the DgN values derived in the present study and those of Wu *et al*.,[3] especially for a 0% glandular breast, may be a consequence of different extrapolation techniques.[2]

Furthermore, to evaluate the DgN values for a desired glandular fraction, Wilkinson and Heggie[23] suggested using the reciprocal interpolation method for interpolating the DgN values between the 0% and 100% glandular fraction rather than using the linear interpolation method as described by Boone,[2] which would reduce interpolation errors from 5% to 1%.

As is known, in a homogeneous breast model, the DgN values increase nearly linearly with decreasing glandular compositions from 100% down to 0% (Fig. 4b). However, in a heterogeneous breast model, the obtained results can be occasionally reversed (Fig. 4a); that is, a smaller fraction of glandular breast does not always result in a higher value of DgN as compared to a larger glandular fraction, especially if the center position of the slab is far below the top surface of the breast. This result corresponds to the work of Zankl *et al*.[10] in which they used breast voxel models segmented from a high resolution computed tomography data set. Zankl *et al*.[10] showed that the glandular tissue is predominantly concentrated in the lower part of the model, and they found that the conversion coefficients (DgN) were lower by up to 40% for the thicker models. Consequently, the spatial distribution of the glandular component of the breast will have a large effect on the overall accuracy of the glandular dose calculation.[9]

The DgN values obtained from using adipose tissue as a superficial layer are 1.12 to 1.36 times greater than those of skin tissue for a thickness of 2 to 6 mm, and for this reason, the results of Dance,[1] who used adipose tissue, are higher than those of this work by around 15%. When the skin thickness is not 4 mm, the DgN values fluctuate from +17%, +8%, –7%, and –13% for 2-, 3-, 5-, and 6-mm skin thickness, respectively, which agrees very well with the results of Boone.[2] Skin thickness is different for each individual, so it is difficult to correctly estimate the glandular dose. For this reason, a skin thickness measurement or evaluation method may be required for an accurate estimation of the glandular dose.

The tissue composition and breast shape and size have little effect on the DgN values. For the thickness of breast support, our results correspond with those of Zoetelief *et al*.[7] in which they suggested that the influence of the backscattering material on the DgN values is about 0.2%; therefore, these factors may not be of concern in the glandular dose simulations when compared to the local distribution of glandular tissue and skin thickness of the breast.

In conclusion, the EGSnrc Monte Carlo package and its associated user codes were used in the simulations because they are efficient and convenient for modeling X-ray tube components of a mammography unit (with BEAMnrc) and for modeling breast voxel phantoms (with DOSXYZnrc). We performed simulations to evaluate and investigate breast dosimetry, particularly emphasizing the average glandular dose in breast models and relevant normalized glandular dose coefficients. Various factors affecting the average glandular dose were also investigated. Although there are several relevant factors in the MC simulation, such as the MC code, tissue composition, and X-ray spectrum, that can affect the results of the simulations (the normalized glandular dose coefficients), we demonstrated that our results are in good agreement with current published works.[2,3] As anticipated, the local distribution of glandular tissue in the breast and the breast skin thickness have a large effect on the estimation of average glandular dose; therefore, it is very important to take these two factors into account when we need a more accurate assessment in breast dosimetry for mammography.[10] However, it is difficult to exactly specify the location of glandular tissue without using a new modality such as MRI, CT, or digital tomosynthesis. In future work, to improve the estimation of average glandular dose, we should study a realistic representation of the glandular tissue in various distribution patterns in the breast for fragments of glandular tissue, with many shapes, sizes, and locations, by using a voxel-based phantom created from CT or MRI data.

ACKNOWLEDGEMENTS

We thank the authors of the EGSnrc Monte Carlo code for the free use of their code, without which this work would not have been possible. One of the authors, N. Phaisangittisakul, would like to acknowledge the partial support from the Thailand Center of Excellence in Physics.

REFERENCES

1. Dance DR (1990) Monte Carlo calculation of conversion factors for the estimation of mean glandular breast dose. Phys Med Biol **35**: 1211–1219.
2. Boone JM (1999) Glandular breast dose for monoenergetic and high-energy X-ray beams: Monte Carlo assessment. Radiology **213**: 23–37.
3. Wu X, Barnes GT and Tucker DM (1991) Spectral dependence of glandular tissue dose in screen-film mammography. Radiology **179**: 143–148.
4. ACR (1999) Mammography quality control manual. Reston, Va: American College of Radiology.

5. Dance DR, Skinner CL and Carlsson GA (1999) Breast dosimetry. Appl Radiat Isot **50**: 185–203.
6. Liu B, Goodsitt M and Chan HP (1995) Normalized average glandular dose in magnification mammography. Radiology **197**: 27–32.
7. Zoetelief J and Jansen JTM (1995) Calculation of air kerma to average glandular tissue dose conversion factors for mammography. Rad Prot Dosim **57**: 397–400.
8. Carlsson GA and Dance DR (1992) Breast absorbed doses in mammography: evaluation of experimental and theoretical approaches. Radiat Prot Dosim **43**(1/4): 197–200.
9. Boone JM (2002) Normalized glandular dose (DgN) coefficients for arbitary x-ray spectra in mammography: computer-fit values of Monte Carlo derived data. Med Phys **29**(5): 869–875.
10. Zankl M, *et al* (2005) Average glandular dose conversion coefficients for segmented breast voxel models. Radiat Prot Dosim **114**(1–3): 410–414.
11. Speiser RC, Zanrosso EM and Jeromin LS (1986) Dose comparisons for mammographic systems. Med Phys **13**(5): 667–673.
12. Delis H, *et al* (2005) The influence of mammographic X-ray spectra on absorbed energy distribution in breast: Monte Carlo simulation studies. Radiat Meas **39**(2): 149–155.
13. Jansen JTM, Wit NJP and Zoetelief J (1992) Comparison of measured and calculated in-phantom depth-dose distributions for mammography. Radiat Prot Dosim **43**(1/4): 245–249.
14. Kawrakow I and Rogers DWO (2003) The EGSnrc code system: Monte Carlo simulation of electron and photon transport. National Research Council of Canada Report PIRS-701.
15. Nigapruke K, *et al* (2009) A comparison of mammographic x-ray spectra: simulation with EGSnrc and experiment with CdTe detector. J Radiat Res **50**(6): 507–512.
16. Walters BRB and Rogers DWO (2003) DOSXYZnrc users manual. National Research Council of Canada Report PIRS-794.
17. ICRU (1989) Tissue substitutes in radiation dosimetry and measurement report 44 (Bethesda, MD, USA: ICRU).
18. Berger MJ and Hubbell JH (1987) XCOM, Photon cross sections on a personal computer, report no. NBSIR87–3597. Gaithersburg MD 20899: NIST.
19. Hubbell JH and Seltzer SM (1995) Tables of X-ray mass attenuation coefficients and mass energy-absorption coefficients 1 keV to 20 MeV for elements Z51 to 92 and 48 additional substances of dosimetric interest. NISTIR 5632.
20. Hammerstein GR, *et al* (1979) Absorbed radiation dose in mammography. Radiology **130**: 485–491.
21. IAEA (2007) Dosimetry in diagnostic radiology: an international code of practice, technical reports series no. 457. International Atomic Energy Agency, Vienna.
22. Doi K and Chan HP (1980) Evaluation of absorbed dose in mammography: Monte Carlo simulation studies. Radiology **135**: 199–208.
23. Wilkinson LE, Heggie JCP and Johnston PN (1999) An investigation into the impact of anatomical variation upon mean glandular dose produced within a standard breast. Australas Phys Eng Sci Med **22**: 53–63.
24. Tucker DM, Barnes GT and Wu XZ (1991) Molybdenum target x-ray spectra: a semiempirical model. Med Phys **18**: 402–407.
25. Boone JM, Fewell TR and Jennings RJ (1997) Molybdenum, rhodium, and tungsten anode spectral models using interpolating polynomials with application to mammography. Med Phys **24**: 1863–1874.

Received on January 18, 2010
Revision received on March 19, 2010
Accepted on March 28, 2010
J-STAGE Advance Publication Date: June 2, 2010